

# **Molecular dynamics simulation of thermal and mechanical properties of polyimide-carbon-nanotube composites**

Dewei Qi and Jeffrey Hinkley<sup>1</sup>

Department of Paper Engineering, Chemical Engineering, & Imaging  
College of Engineering and Applied Science  
Western Michigan University, Kalamazoo MI 49008

<sup>1</sup>Advanced Materials and Processing Branch, NASA Langley Research Center, MS 226, 6A West Taylor Street, Hampton, VA 23681

## **Abstract**

An aromatic polyimide and its mixture with randomly distributed carbon nanotubes are simulated by using molecular dynamics, repeated energy minimization and cooling processes. The glass transition temperatures are identified through volume-temperature curves. Stress-strain curves, Young's moduli, volumes and Poisson ratios at different temperatures are computed at different temperatures. It is demonstrated that the carbon nanotube reduces the softening effects of temperature on mechanical properties and increases the ability to resist deformation.

## **Introduction**

With the recent development of nano-technologies, it is hoped that polymer composites can be reinforced by adding carbon nanotubes. Various polymers can be used to make composites. Frankland et. al. [1] simulated and modeled the stress-strain behavior of polyethylene-nanotube composites using molecular dynamics (MD). They found that long carbon nanotubes, but not short ones, could reinforce mechanical properties.

One interesting polymer is LARC-SI(NASA Langley Research Center Soluble Imide) [2, 3] which is a wholly aromatic thermoplastic copolyimide. Aromatic rings in polymers tend to give better mechanical and thermal properties and good environmental resistance. This polyimide has high adhesive strength and can be mixed with carbon nanotubes to produce stiff, and light weight composites. Park et. al. [4] experimentally studied the mechanical properties of polyimide/single wall carbon nano-tube composites. They found that the storage modulus is increased by 65% when 1% of carbon nano-tubes in volume was added. In the present work, we construct the aromatic copolyimide (LARC-SI) and its composites with single-walled carbon nanotubes (NT) and investigate temperature effects on the stress-strain behavior.

Generally speaking, there are two methods that can be used to simulate the mechanical properties. One is called molecular mechanics [5-7]. In this method, the potential energy of the system is minimized and the stresses are computed under straining. Essentially, the energy minimization corresponds to a system at the temperature  $T=0$  K. Therefore, this method cannot be used to examine the temperature effect. Another method is molecular dynamics simulations. The MD method can be used to investigate how physical properties vary with temperature and time. In the present work, we conduct several MD simulations to study how carbon nanotubes affect the mechanical properties of polyimide composites and how temperature affects the tensile-strain curves of polyimide-nanotube composites. Since the molecular structure of LARC-SI, as shown in figure 1, is much more complex than polyethylene, special efforts are required to construct LARC-SI polymers.

Section two briefly describes the simulation method. Section three expresses the method of construction of LARC-SI polymer composites and polyimide-carbon-nanotube composites. This section also presents detailed

simulation procedures. Section four presents results and discussion. The final section summarizes our conclusions.

### Simulation method

Molecular dynamics simulations are used to model the mechanical properties of carbon nanotube polymeric composites. The well known Tripos 5.2 force field [8] is adopted in this work. It was extensively demonstrated by other authors [9] that the Tripos 5.2 force field is accurate for polyimides and aromatic polymers that have 5-membered and 6-membered ring structures. A parallel code called LAMMPS [10] is employed. The code of Tripos 5.2 force field is written and added to the LAMMP by the present authors. The total potential energy is expressed as

$$V_p = \sum_{bonds} V_b + \sum_{angles} V_a + \sum_{torsions} V_t + \sum_{outofplane} V_o + \sum_{nonbonds} V_{nb}$$

The first term in the right hand of the above equation is

$$V_b = k_b (r - r_0)^2$$

where  $k_b$  is the bonding energy parameter,  $r_0$  is the equilibrium bonding distance;  $r$  is the actual bonding distance. The second term is the bending potential and is written

$$V_a = k_a (\theta - \theta_0)^2$$

where  $k_a$  is the angle energy parameter;  $\theta$  the bending angle; and  $\theta_0$  the equilibrium angle. The third term is the torsion potential written as

$$V_t = k_t \left[ 1 + \frac{S}{|S|} \cos(|S| \phi - \phi_0) \right]$$

where  $k_t$  is the torsion energy constant;  $\phi$  is the torsion angle;  $\phi_0$  is the equilibrium torsion angle. The fourth term is the out-of-plane bending potential that can be denoted by

$$V_o = k_o d^2$$

where  $k_o$  is the out-of-plane bending force constant and  $d$  is the distance from an atom to the plane defined by its three attached atoms. The last term is nonbonding energy and the Leonard-Jones 6-12 potential (L-J) is used,

$$V_{nb} = 4\epsilon \left[ \left( \frac{\sigma}{r} \right)^{12} - \left( \frac{\sigma}{r} \right)^6 \right],$$

where  $\epsilon$  is the depth of the energy well;  $\sigma$  is radius of the atom.

In the following sections, we will construct models of carbon NT crystals, LARC-SI polymer and its mixtures with single-walled carbon NT.

### LARC-SI polyimide -carbon-nanotube composite

First, we use computer to construct a carbon NT crystal as shown in figure 1. The axes of tubes are set along the z-direction of a simulation box and the tubes form a triangular close-packed crystal lattice in the x-y plane with a lattice constant  $2r+l$  where  $r$  is the tube radius and  $l$  is the intertube separation. There are 18 carbon nanotubes and 3024 atoms in the simulation box as shown in figure one. All NT in this crystal are single-

walled and denoted by (n=4,m=4). The (n,m) notation refers to the chiral vector of the NT in terms of the primitive in-plane lattice vectors of a graphene sheet [11]. The radius of (4,4) NT is  $r=2.71 \text{ \AA}$  and  $l=3.15 \text{ \AA}$  initially. We call this type crystal a (4,4) crystal.

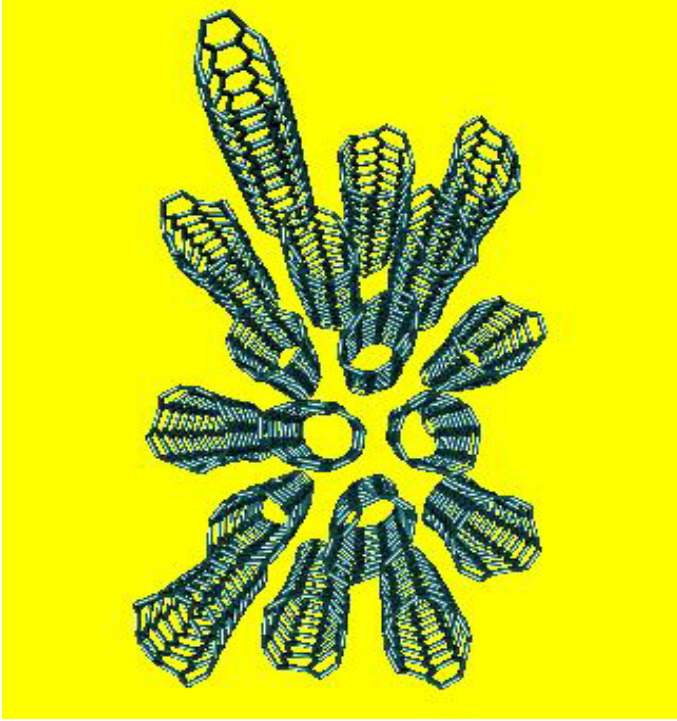


Figure 1. Carbon nanotube (4,4) crystal with 18 tubes in the simulation box at  $T=293 \text{ K}$ .

Aromatic carbon-carbon bonding parameters in the Tripos 5.2 Force field are applied to carbon-carbon bonds of a NT. The equilibrium bonding distance in the NT is replaced by its experimental value  $1.42 \text{ \AA}$ . The validation of the parameters for the NT is examined by computing Young's modulus.

MD simulations are run at pressure  $p=1$  atmosphere (atm) and temperature  $T=293 \text{ K}$  for  $120 \text{ ps}$  by using the Nose-Hoover algorithm [12-13]. The time step is  $1 \text{ fs}$  and the cut off distance for non-bonded interactions in the crystal is  $10 \text{ \AA}$ . Periodic boundary conditions are imposed for all the MD runs in this work. Then the system is cooled from  $T=293$  to  $T=10 \text{ K}$  by scaling velocities at a constant cooling rate of  $-1.96 \text{ K/ps}$ . After the temperature arrives at  $T=10$ , the system is run for  $30 \text{ ps}$ . Next, the average dimensions of the simulation box are measured over another  $30 \text{ ps}$ . Subsequently, the crystal is stretched at  $T=10 \text{ K}$  by decreasing the external applied pressure in the z-direction or tube axis-direction at a constant rate  $\alpha_z = \Delta p / \Delta t = -250 \text{ atm/ps}$ . Here  $\Delta p$  is the pressure change and  $\Delta t$  the stretching time increment. The external pressure is held constant at  $p=1 \text{ atm}$  in the x- and in the y-directions. The stress in response to the external tension is measured during stretching by

$$\frac{1}{V} \sum_i (m_i v_i v_i - F_i r_i)$$

where  $V$  is the volume;  $v_i$  is velocity;  $m_i$  is the mass;  $F_i$  is force;  $r_i$  is the position. The stresses and dimensional changes of the simulation box are recorded during stretching. Young's modulus could be calculated through the stress-strain curve. This method was first used by Brown and Clarke [14] and a similar method was also reviewed by Ray [15].

The calculated stress  $\sigma_z$  as a function of strain  $\epsilon_z$  is plotted in figure 2. Each point in the figure is an average value over  $1 \text{ ps}$  time interval. The slope of linearly fitted line represents Young's modulus. We obtain Young's

modulus  $E_z=1.30$  TPa for this (4, 4) crystal. The same method is applied to a (10, 10) crystal and produces Young's modulus  $E_z=0.89$  TPa.

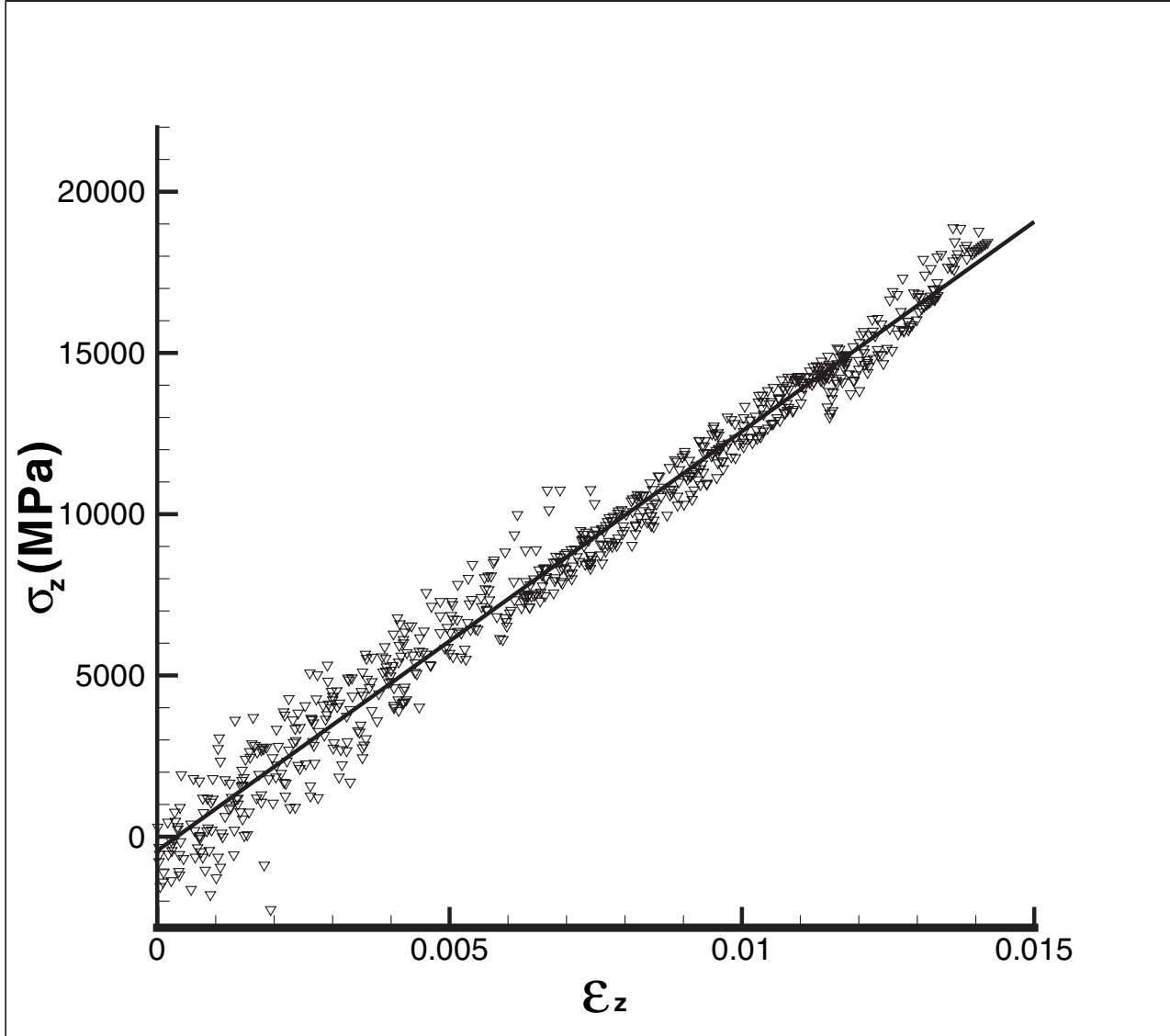


Figure 2. The stress in the NT axis direction as a function of strain for (4,4) NT crystal. Each point is an average value over 1ps time interval.

Laboratory measurements of the amplitude of the intrinsic thermal vibrations of the tubes yield an average value of 1.8 TPa with a very large variation [16]. Experimental bending measurements on Young's modulus give an average value of  $1.28 \pm 0.59$  TPa while recent tight-binding calculations produce a value of the order of 1 TPa [17]. It is clear that presently calculated Young's moduli are located within the same range as other authors'. In addition, the radius of the (10, 10) NT is 6.78 Å and larger that of the (4, 4) NT. Young's modulus reduces as the radius of tube increases. This trend [18] is correctly caught by our simulations. Therefore, we are confident that the Tripos force field 5.2 is suitable for computations of mechanical properties of carbon NT.

Now we turn attention to polyimide composites. The molecular structure of LARC-SI polymer with one basic unit is shown in figure 3. Note that the 50:50 copolymer is shown as strictly alternating, which is probably a simplification. The asymmetric diamine 3,4' oxydianiline can insert in the chain in two directions; this minor structural detail is ignored.

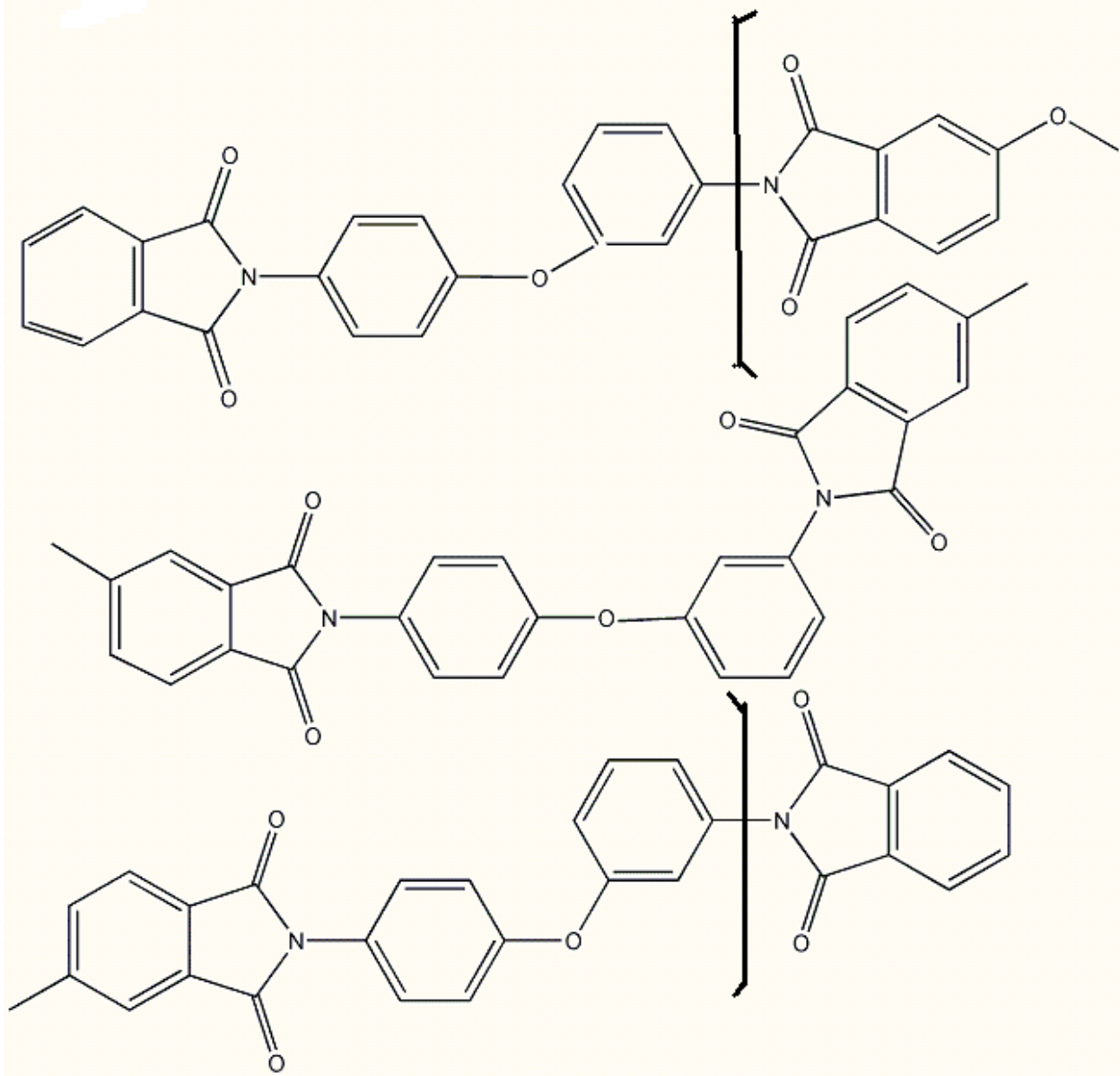


Figure 3. Chemical structure of LARC-SI polyimide.

Since amorphous composites have more complex structure than crystals, a variation of a Monte Carlo method [19] called POLY-PIC has been developed to construct composites of LARC-SI polymers and carbon NT. In our code, a five- or six- membered ring with equilibrium positions and angles is pre-constructed in a plane in a body-fixed coordinate system. The pre-constructed rings are sequentially connected together one by one. Three Euler angles are used to control the orientation of one ring connecting to other ring or to other atom through the three random numbers. Coordinate transfers from the body fixed coordinates system of each ring to a space fixed coordinate system are used for each connecting. Simultaneously the distances between any two nonbonded atoms are checked during connecting. Whenever the distance between the two atoms is less than a preset value, say 1.8 Å, we delete the added ring or atom and assign new random numbers to this ring or atom. If the distance is still smaller than the preset value after many iterations, then the entire molecule is deleted and reconstructed.

Three different composites were constructed. In the first structure, illustrated in figure 4, there are 8 LARC-SI molecules and no carbon NT. Each molecule has 6 repeated units (645 atoms). The total number of atoms is 5160.

We use and accept the concept that solid amorphous materials after cooling from their liquid state will keep the same structure as the liquid state. This well-known concept for L-J glasses is applied to composites. Therefore, we initially construct a polyimide melt with a density of  $\rho=0.688 \text{ g/cm}^3$ .

The second structure consists of 7 LARC-SI polyimide molecules and one carbon NT. The carbon NT with a periodic condition is first placed along the z-direction in the center of the simulation box and goes through the simulation box. The number of carbon atoms in the tube is 546. This carbon nanotube thus corresponds to an infinitely long tube. Next 7 LARC-SI molecules are randomly distributed by using POLY-PIC. Each polymer chain in the composite is the same as that in the first composite. The total number of atoms in the second model composite is 5061, and the nanotube comprises 16% of the weight. The initial density is  $\rho=0.695 \text{ g/cm}^3$ . We simply call the second structure an infinitely-long-tube composite. A snapshot of the second composite is illustrated in figure 5.

The third composite in the simulation is designed as 10 short carbon NT mixed with 25 LARC-SI polyimide molecules as demonstrated in figure 6. The length of each carbon NT is 95.86 Å. Each LARC-SI polyimide molecule is the same as that in the first and second structures. Each carbon (4,4) tube has 616 atoms. POLY-PIC constructs the composite by randomly either adding NT or constructing molecules. The total number of atoms is 22,285 and the NTs are 33 % by weight in the third composite. The initial density is  $0.354 \text{ g/m}^3$ . Since the length of carbon nanotubes in the third composite is not infinite, we call the third composite a short-tube composite.

From these initial configurations, we run constant pressure MD simulations at  $p=1 \text{ atm}$  and  $T=1000 \text{ K}$ . The cut off distance for unbonded interactions for composites is 15 Å. Essentially, each composite is compressed from its initial size to its equilibrium size.

The LARC-SI polymers are melted at this high temperature  $T=1000\text{K}$  far above the glass transition temperature  $T_g = 522\text{K}$  [20] to ensure the composite having a random structure. Fan et al [5] used molecular dynamics simulation and repeated energy minimization method to generate well relaxed aromatic polysulfone and polycarbonate. This method has been extensively used to correctly create amorphous structures in a computer by many authors [6-7]. Following their work, we relax each composite initially for a total of 150 ps, at least,

then alternately minimize energy using Hessian-free truncated Newton method and perform 60ps MD runs. There are 6 minimization/MD cycles, in total, to ensure a relaxed structure.

/

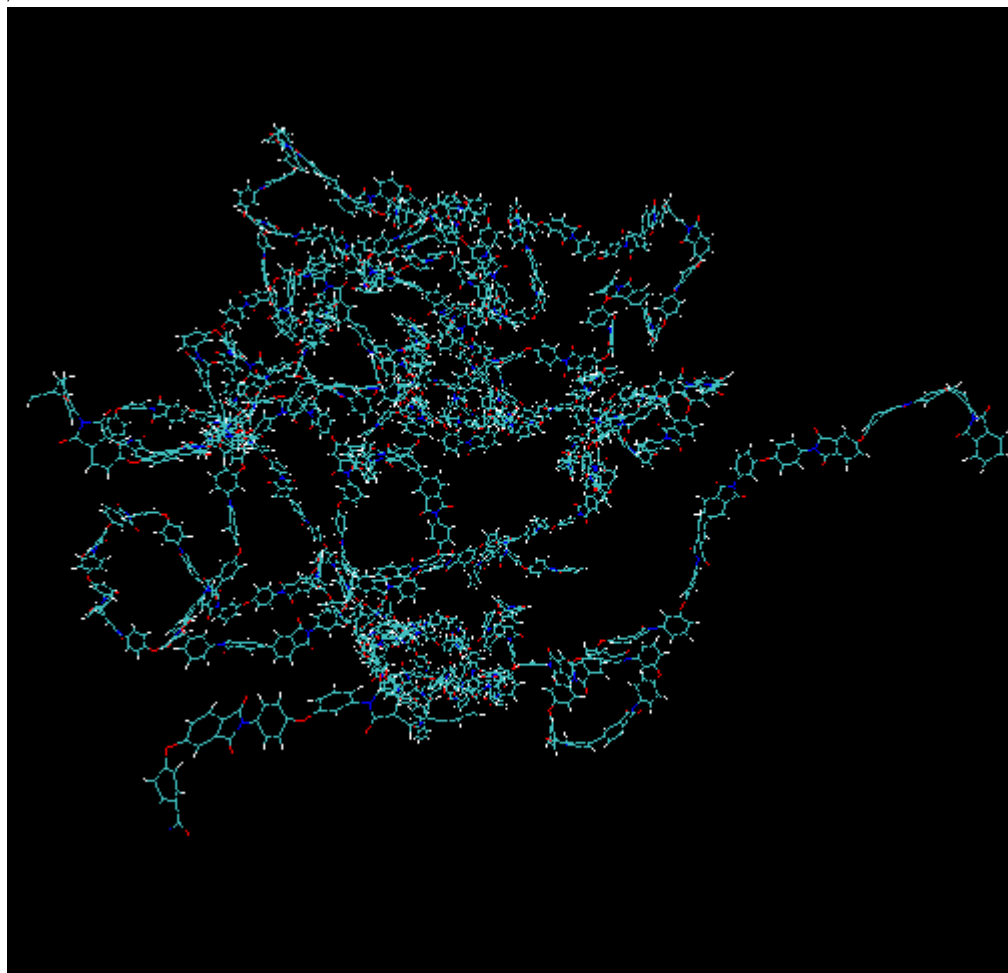


Figure 4. A polyimide composite consists of 8 LARC-SI polymers. The simulation box is not shown.

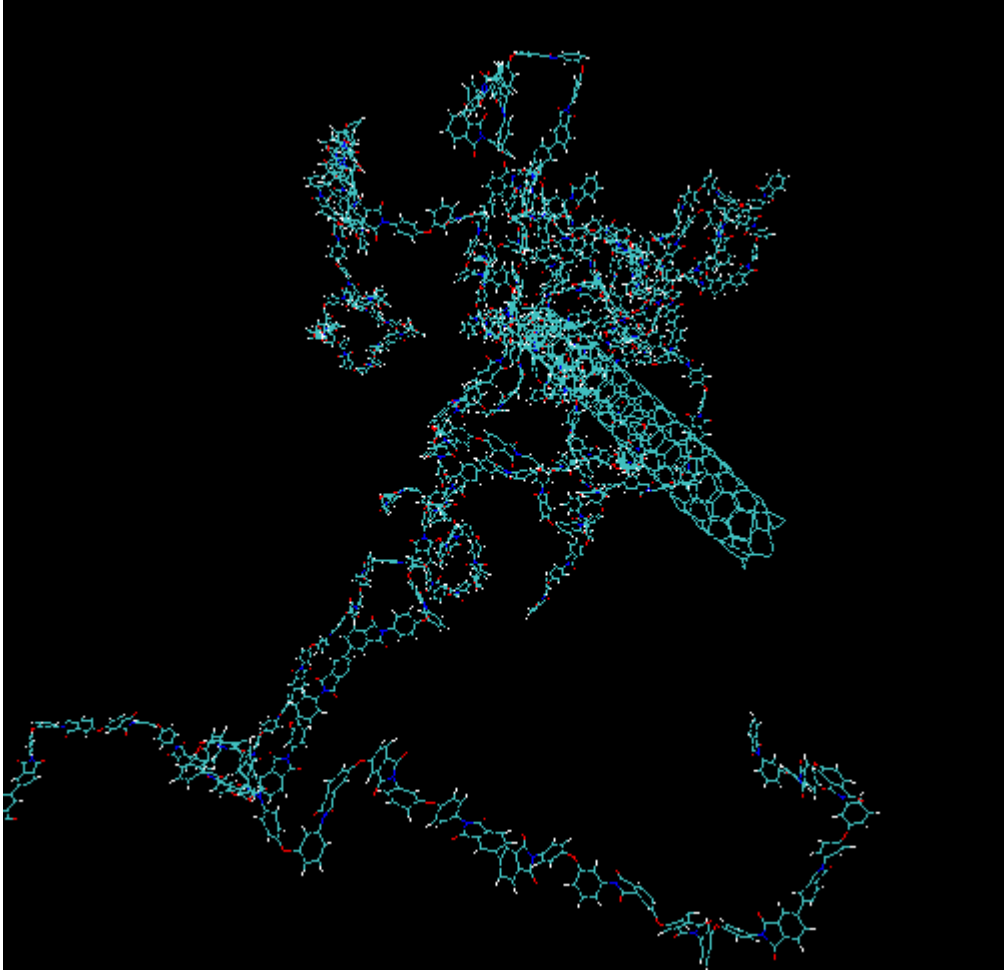


Figure 5. Polyimide-ininitely-long-tube composite consists of 7 LARC-SI polymers and a single-ininitely-long nano-tube.

Next, the composites are cooled from  $T=1000$  K to lower temperatures at a constant cooling rate of  $-1.96\text{K/ps}$ . Configurations at interest temperatures are recorded during the cooling process. Starting from the recorded configurations, the assemblies are run for 30ps at the corresponding temperatures and at  $p=1$  atm to reach an equilibrium state. We relax simulation box size in the x-, y- and z-directions independently during MD runs. In other words, the lengths in the three directions should be independently varied without tension coupling. Therefore, although the initial simulation box is a cube, the final simulation box lengths in the three directions may be different. The final density at room temperature  $T=293$  K is  $1.21\text{g/cm}^3$  for the polyimide composite,  $1.23\text{ g/cm}^3$  for the infinitely-long-tube composite and  $1.35\text{ g/cm}^3$  for the short-tube composite.



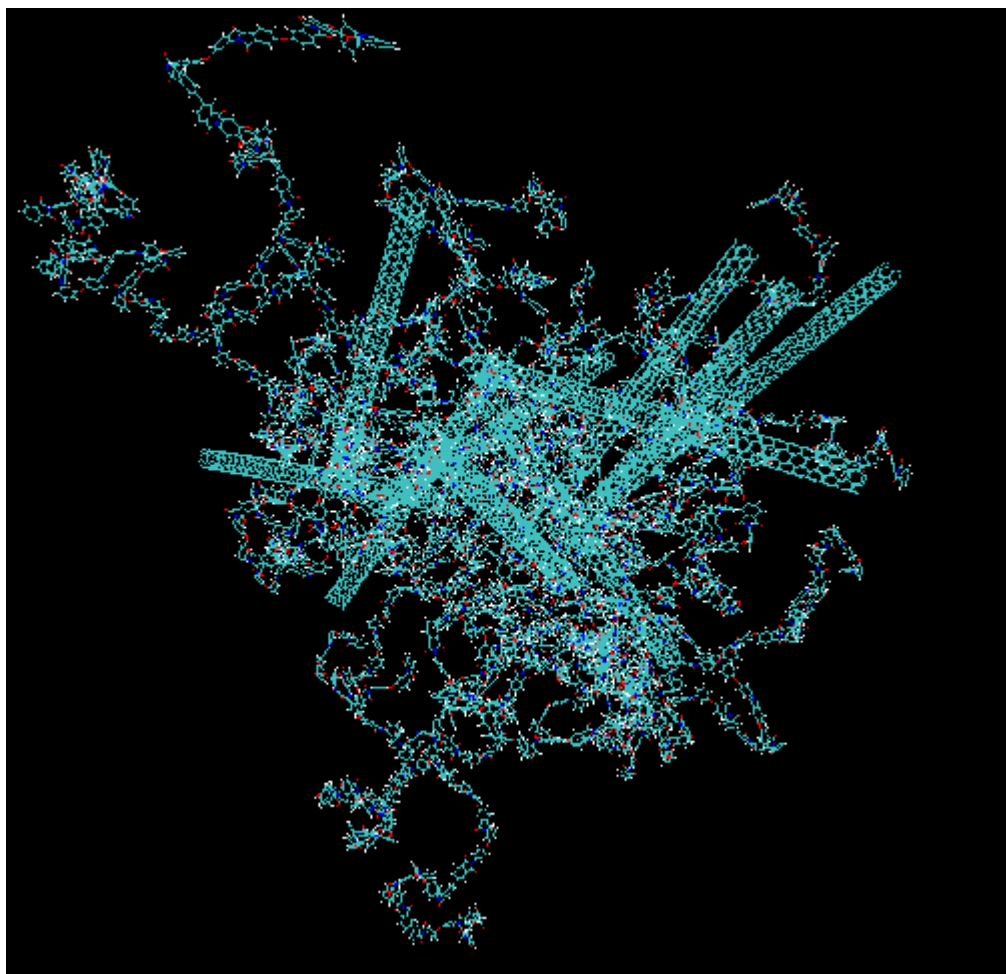


Figure 6. The polyimide-short-tube composite consists of 25 LARC-SI polymers and 10 nanotubes.

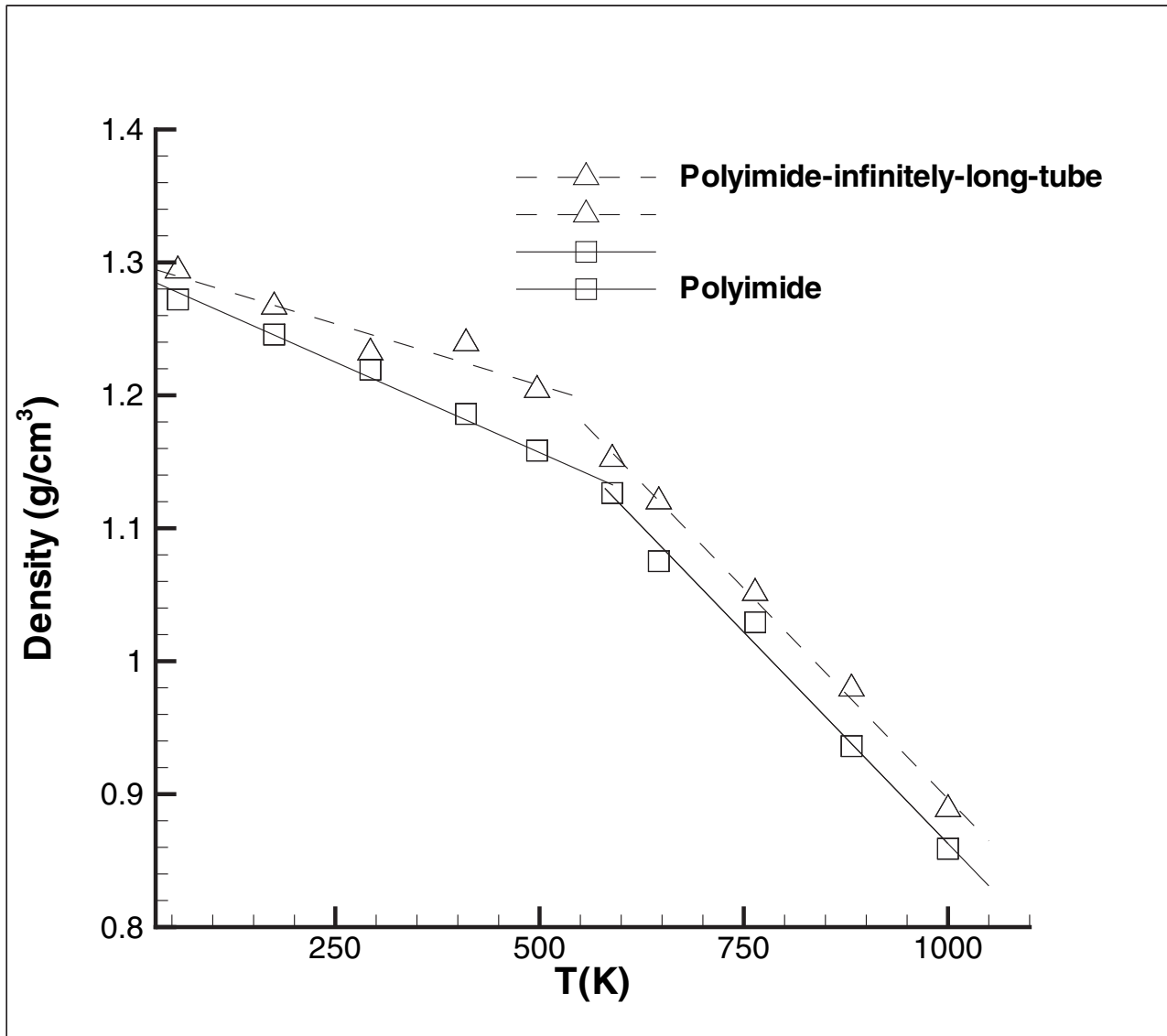


Figure 7. The densities as functions of temperatures for the polyimide composite (squares) and the polyimide-infinitely-long-tube composite (triangles). The curves are divided into two parts, each part is linearly fitted. The glass transition point is identified by the intersection of the two lines.

### Simulation results and discussion

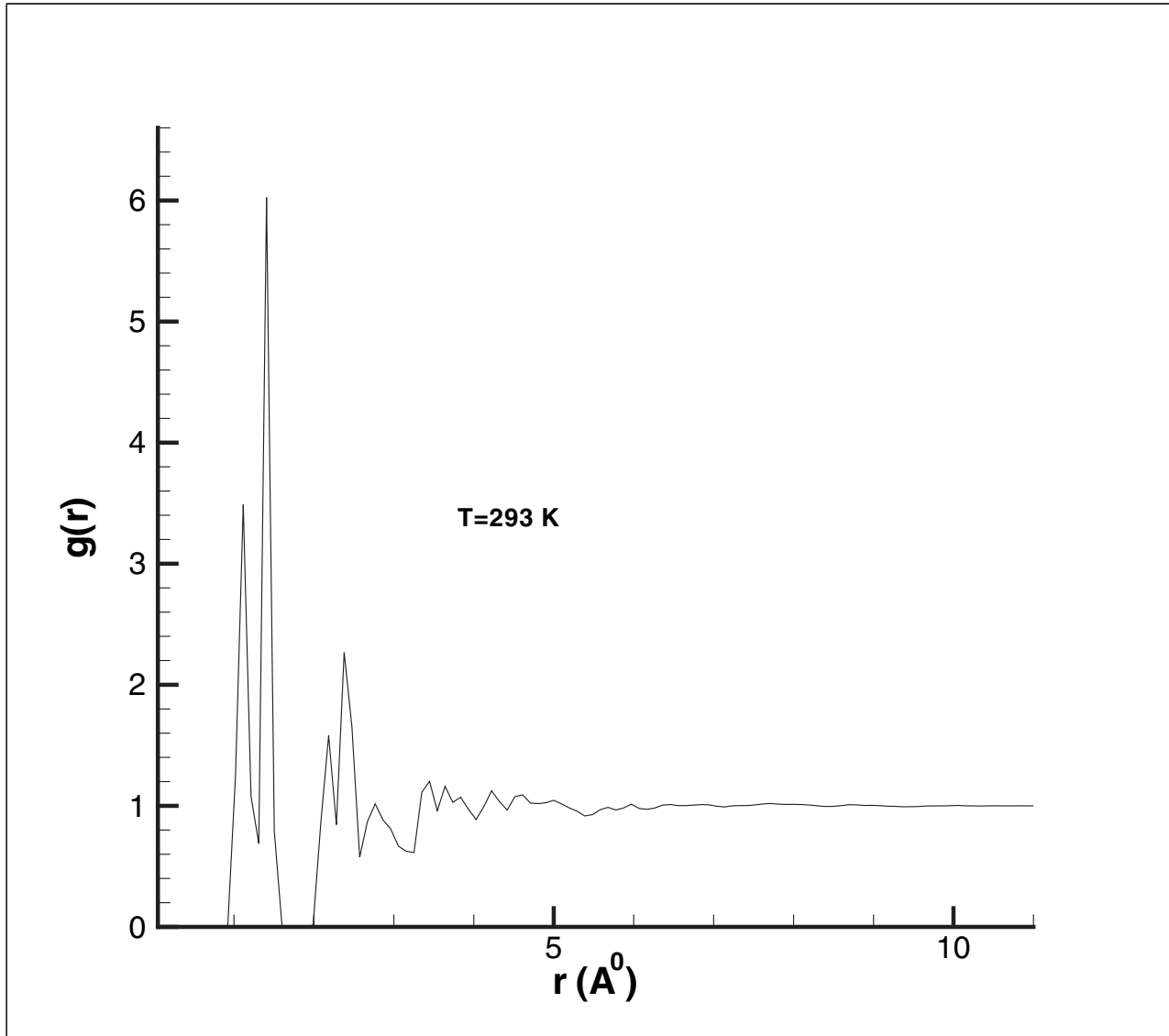


Figure 8. A radial distribution function  $g(r)$  of LARC-SI at  $T=293$  K.

For composites, after repeated energy minimizations and molecular dynamics runs, we obtained a well relaxed amorphous structure. A radial distribution function (RDF)  $g(r)$  for all atoms of LARC-SI at  $T=293$  is plotted in Figure 6. The first peak in the RDF corresponds to the distance between of hydrogen and carbon atoms and the second peak corresponds to the distance between carbon and carbon atoms in the rings. When  $r > 5$  Å, RDF becomes flat and approaches 1.0, demonstrating that the materials lacks long range orders and posses the characteristic of amorphous structure. In addition, energy minimizations can effectively reduce torsional energy, as reported before [5]. In our simulations, dihedral energies are reduced quickly in the minimization processes. We observe no significant high-energy torsional states.

It is well known that for an amorphous L- J system a glass transition can be identified from the density-temperature curve. Linear fitting for both the super cooling liquid region and the solid region can be used to find an intersection corresponding to a glass transition. We apply this knowledge to molecular dynamics simulations of the polymer systems. The density at the constant pressure  $P=1$  atm is an average over 30ps at a given temperature. The results of the density as a function of temperature are plotted in figure 7 for both the polyimide and the polyimide-infinitely-long-tube composite. There are two portions that could be linearly fitted

in each curve. The intersection of the two lines gives a glass transition temperature  $T_g = 570\text{K}$  for the polyimide composite and  $T_g = 550\text{K}$  for the polyimide-infinitely-long-tube composite. The transition temperature for the former composite is only 40 K higher than the experimental result [2, 20]. This result is not surprising because we have used a very high cooling rate. A higher cooling rate leads to a higher glass transition temperature. We observe that the slope of the line above  $T=570\text{K}$  is larger than that below  $T=570\text{K}$ . It is clear that the slope in the solid region is smaller for the polyimide-infinitely-long-tube composite than for the polyimide. In other words, volume thermal expansion coefficient has been reduced by adding carbon NT.

The results of stress-strain curves in the z-direction are plotted in figure 9 for the polyimide assembly and in figure 10 for the short-tube composite. The stress-strain curves in each of the three directions are similar. (The curves in other directions are not shown.)

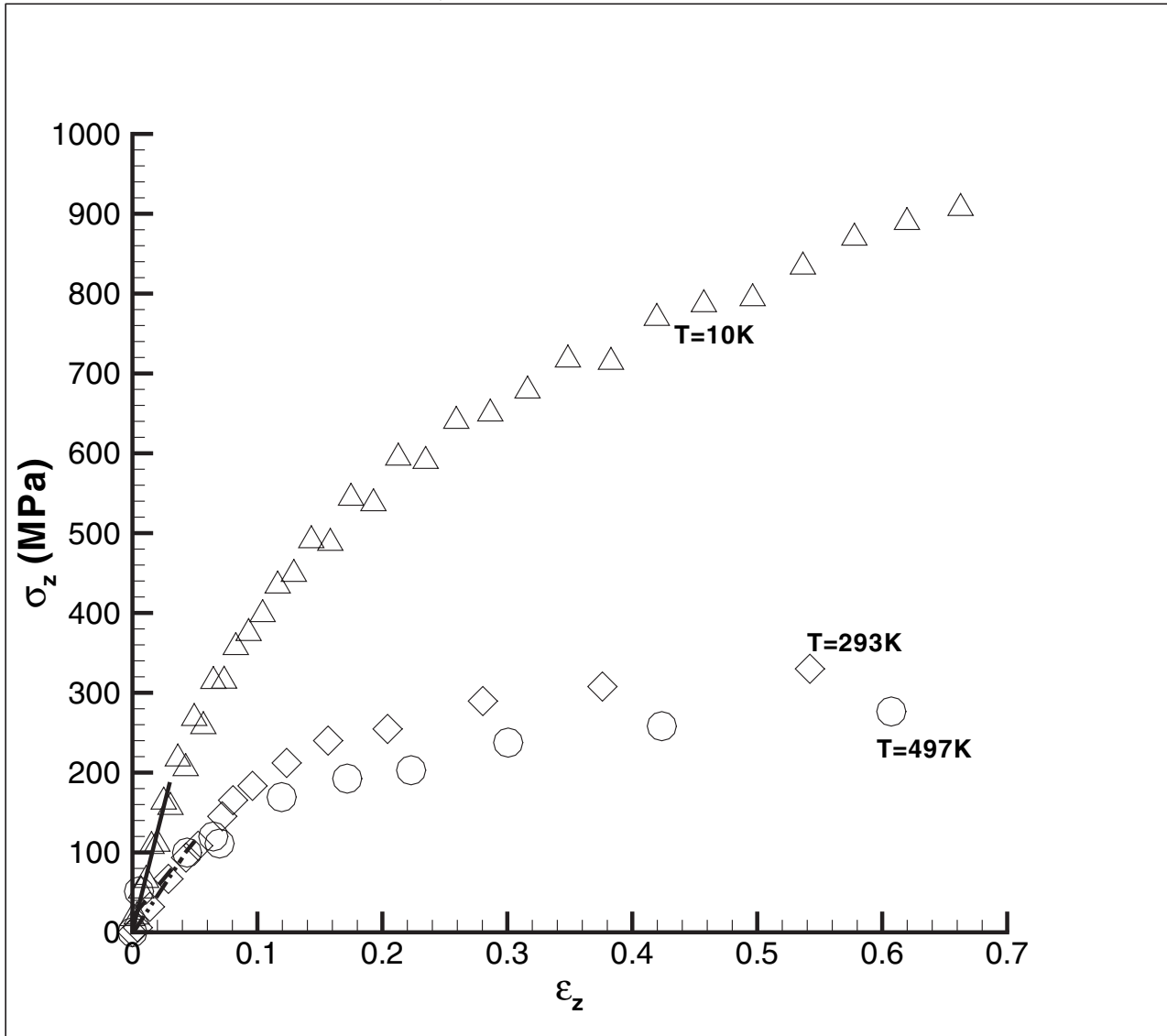


Figure 9. The stress-strain curves in the z-direction for un-reinforced polyimide at  $T=10\text{K}$ ,  $293\text{K}$  and  $497\text{K}$ .

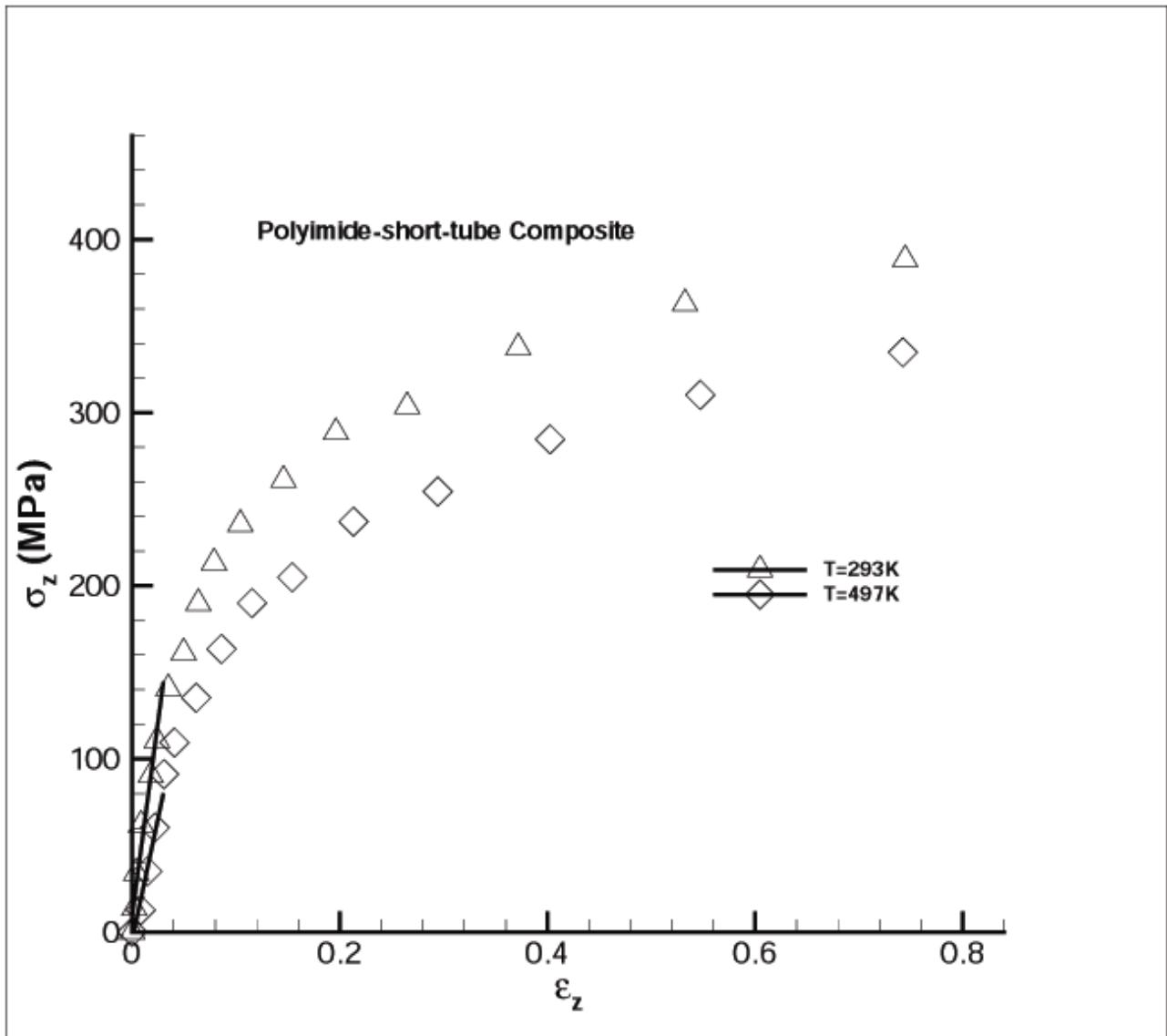


Figure 10. The stress-strain curve for the short-tube composite at T=293K and T=497K.

It is seen that for both the un-reinforced polyimide and the short-tube composite the curves deviate from linearity around strain  $\epsilon_z = 0.08$ . The plastic properties (nonlinear portions) vary with temperature.

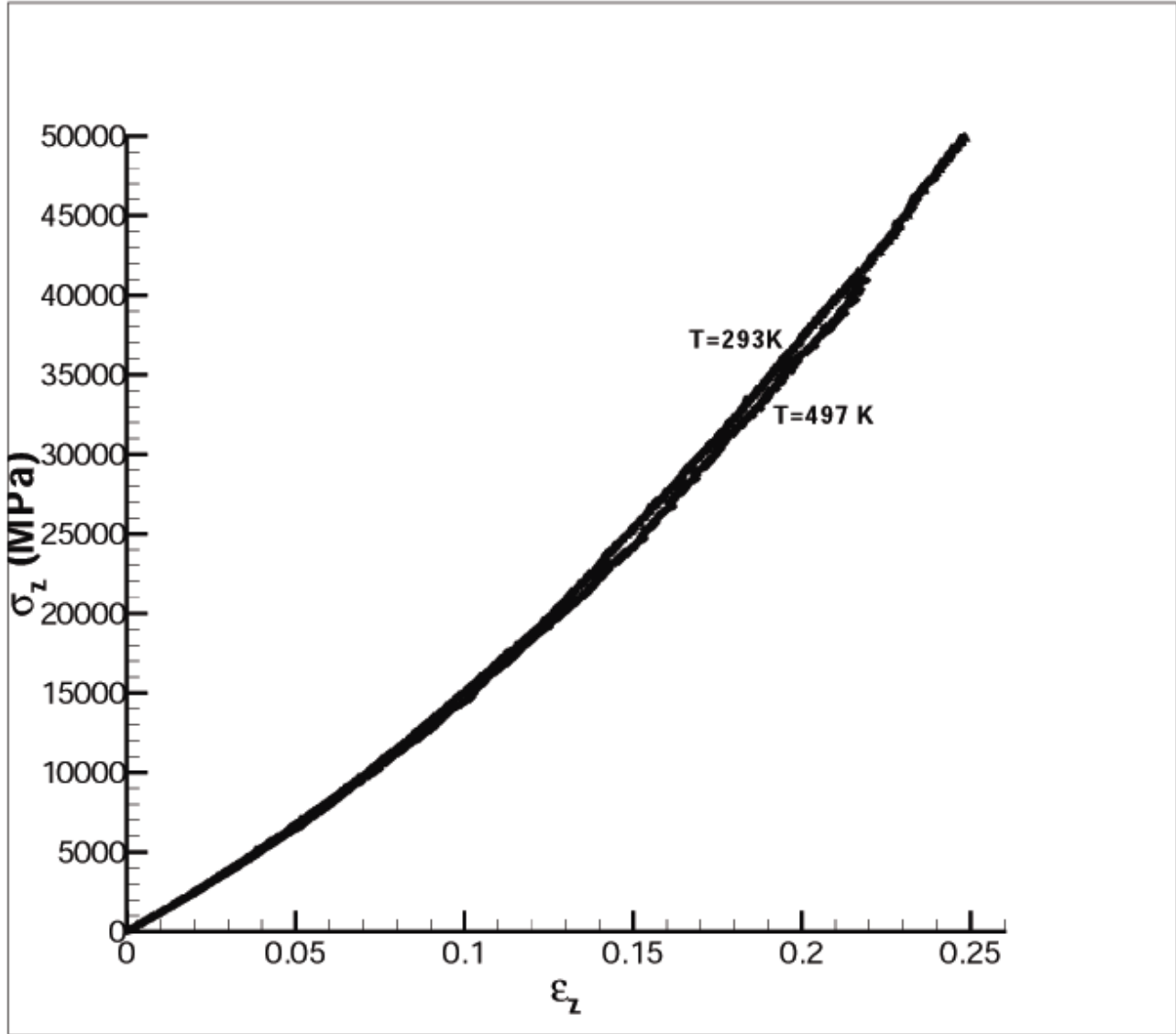


Figure 11. The stress-strain curves in the z-direction for infinitely-long-tube composite at T=293K and T=497K.

To reduce effects of fluctuations, we obtain each point in these figures by averaging MD results of stresses and strains over every 1ps time intervals during stretching. Young's modulus is obtained by a linear fit to the portion of the strain-stress curve up to strain  $\epsilon = 0.04-0.05$ .

Young's modulus for the isotropic un-reinforced polyimide, obtained by averaging in the x-, y- and z-directions, is  $E=2.368$  GPa at T=293K. This is 36% lower than experimental value 3.7 GPa [20]. We note that the simulation density  $\rho = 1.21 \text{ g/cm}^3$  at T=293K was 12% less than the experimental result  $1.376 \text{ g/cm}^3$  [2, 20]. This is partially attributable to the low polyimide molecular weight in the simulation, only 6057. In the experiments the molecular weight is at least 15880 [20]. In addition, we have neglected Coulomb interactions, which might be expected to make a contribution to the energy due to existence of oxygen and nitrogen atoms in the polymers. We are currently working on a simulation including the effects of Coulomb interaction. Therefore, the present results for the model polymer composite are reasonable and still better than those reported by Hu et. al. using molecular mechanics. Their results for Young's modulus for polyimide are 2 times larger than experimental results [6].

As the temperature decreases from  $T=293\text{K}$  to  $T=10\text{K}$ , the Young's modulus increases from  $E=2.37\text{ GPa}$  to  $E=6.27\text{ GPa}$ . When the temperature increase to  $T=497\text{K}$ , the Young's modulus decreases to  $E=1.63\text{GPa}$ . The composite becomes stiffer at a lower temperature. In other words, an increase in temperature can soften the composite, as expected.

The infinitely-long-tube composite is highly anisotropic due to the carbon NT aligned in the z-direction. The stress-strain curves in the z-direction are shown in figure 8 and those in the y-direction in figure 9. Anisotropic behavior is clearly seen by comparing the two figures.

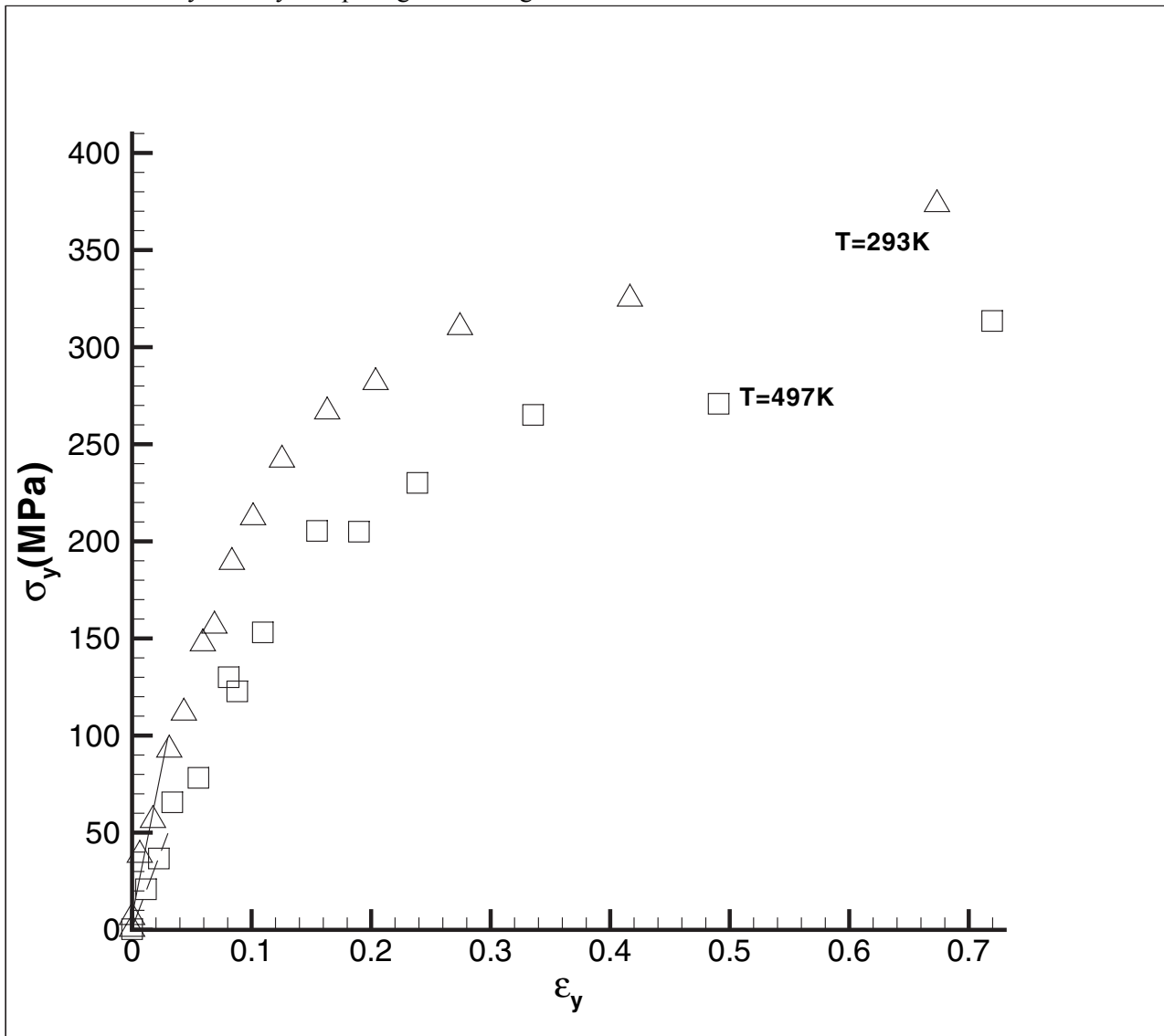


Figure 12. The stress-strain curve in the y-direction for the infinitely-long-tube composite.

We measure the stress-strain curves and Young's modulus in the tube direction or the z-direction and in the transverse directions or the x- and y-direction, respectively. The Young's modulus in the transverse direction is an average of those in the x- and y-directions.

The z-direction stress-strain curves in the infinitely-long tube composite in figure 8 are significantly different from those in the isotropic systems. First, the slope of the linear portion is much larger. Young's modulus in the tube direction is 135 GPa at T=293K and 129 GPa at T=497. These values are 57 and 79 times larger than that of the polyimide without any carbon nanotube at these two respective temperatures, evidencing that mechanical property in the z-direction is greatly enforced by the single carbon NT and such the reinforcement effect is stronger in a higher temperature than in a lower temperature. However, we have to keep in mind that the situation for an infinitely long NT is entirely different from that for a finitely long NT. The infinitely long tube delivers mechanical properties directly to the composite through tube itself, while a finitely-long tube imparts the mechanical properties depending on loading transfers between nanotube and polymers. The longer the NT the larger the loading transfers. This is why Young's modulus in the infinitely-long tube composite is increased much larger than that in the short-tube composite. Second, the shape of the stress-strain curve in infinitely-long-tube composite is entirely different from that in other two systems studied. The curve is slightly concave for the infinitely-long tube composite and more straight; no clearly-defined nonlinear portion appears. Third, the temperature softening effect on Young's modulus is much weaker for the infinitely-long tube composite than for the neat resin. Young's modulus decreases only 4% between 293 K and 497 K (to 129 Gpa). This is in contrast to the 31 % over the same temperature range for the un-reinforced polyimide. The behavior of the stress-strain curve in the y-direction or the transverse direction for the infinitely-long-tube composite in figure 9 resembles that in figures 6 and 7. At T=293 K, the Young's modulus in the transverse direction is 4.12GPa for the infinitely-long-tube composite (compared to 2.37GPa for the neat polyimide ). Although the infinitely-long nanotube reinforces the modulus in the transverse direction, the effect is not as strong as in the tube direction.

Since the stress-strain curves and Young's modulus may depend on the stretching or tension rates, the effects of tension rates on Young's modulus were examined. Stress-strain curves for the polyimide at two different tension rates are shown in figure 13. The higher tension rate  $\alpha_z=250$  atm/ps is 16.66 times larger than the lower tension rate while the Young's modulus at T=293K, calculated from the linear portion of stress-strain curve, is only 16.36% larger than at the lower tension rate. In other words, 16.66 times difference in the tension ratio results in only 16% difference in Young's modulus ratio, indicating the Young's modulus is not very sensitive to tension rate.

In this work we focus on how mechanical properties are enforced by carbon nanotubes, we are more interested in the relative strength increase, not in the absolute values. The errors from the tension rates are not a serious problem as long as we use the same tension when we compare the results of mechanical properties.

Due to a very high stiffness of the infinitely-long-tube composite, the total time to produce the strain up to 21% at T=293K, in figure 9, even at a higher tension rate  $\alpha_z=250$ atm/ps, is 2700ps. This long period in the stretching process dramatically increases the computation time.

Also, from Figure 13, we find that flocculation of stress and strain is smaller at a higher tension rate than at a lower tension rate. For these two reasons, therefore, we use the higher tension rate at  $\alpha_z=250$  atm/ps for all the stretching this work.

For the short-tube composite, the stress-strain curves in the x-and y-directions are similar to the z-direction curves and are not shown here. The Young's moduli derived from the linear portions of the curves are 3.95 GPa at T=293K and 2.88GPa at T=497K, 1.5 times and 1.4 times larger, respectively, than those in the neat polyimide .



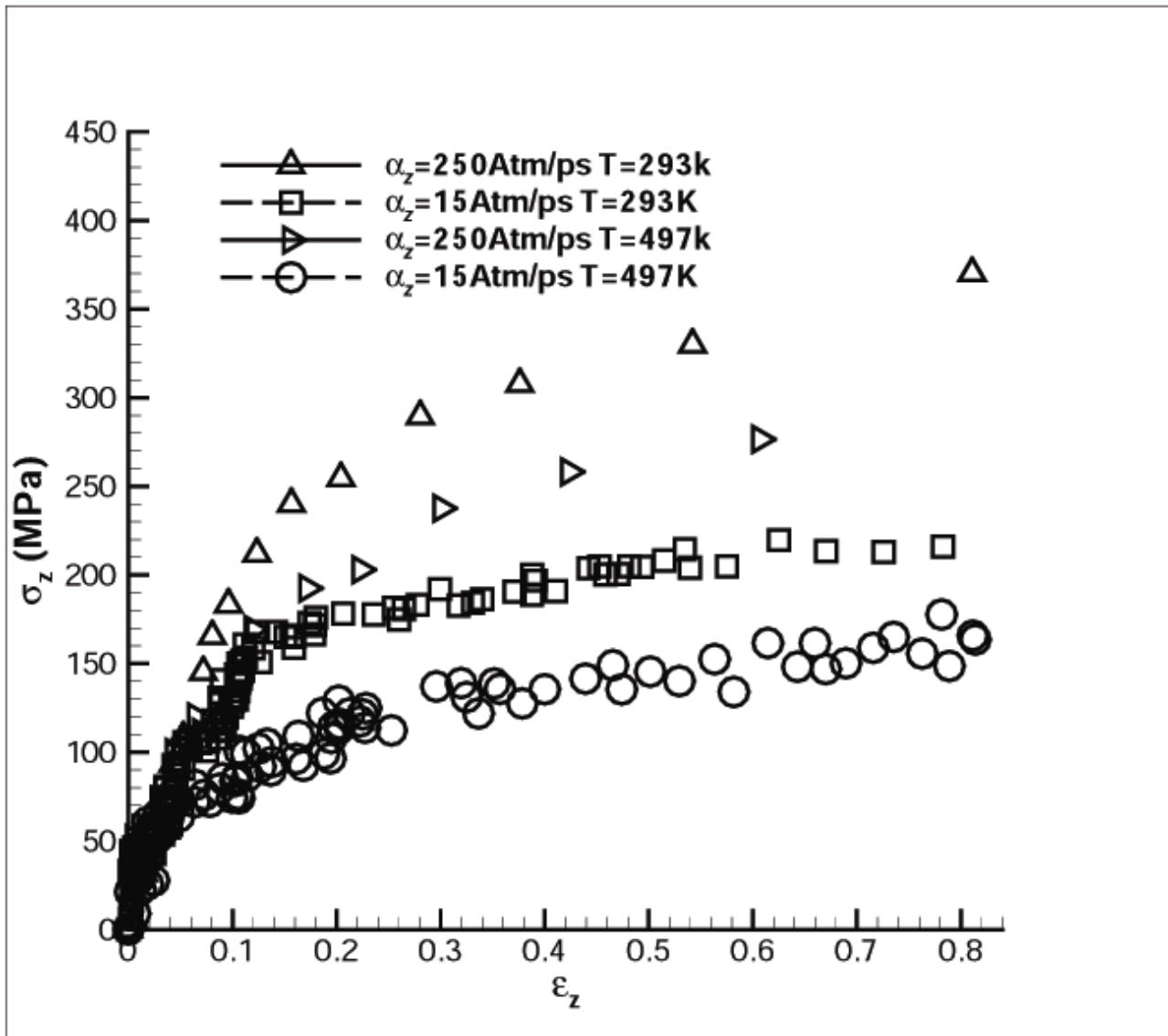


Figure 13. The stress-strain curves at two different tension rates  $\alpha_z = -250$  atm/ps and  $\alpha_z = -15$  atm/ps for the polyimide composite at  $T = 293\text{K}$  and  $T = 497\text{K}$ .

It is interesting that we plot the density as a function of strain  $\epsilon_z$  during stretching for all the three different composites. It is shown that the density of the polyimide and the short-tube composites decreases as strains increase (Figure 14), indicating that stretching increases their average atom distance. The density of the infinitely-long-tube composite, on the other hand, stays at the same level (with some fluctuation). The total volume of the infinitely-long-tube composite is not dramatically changed, suggesting that this materials has a much higher ability to resist the deformation than other two materials.

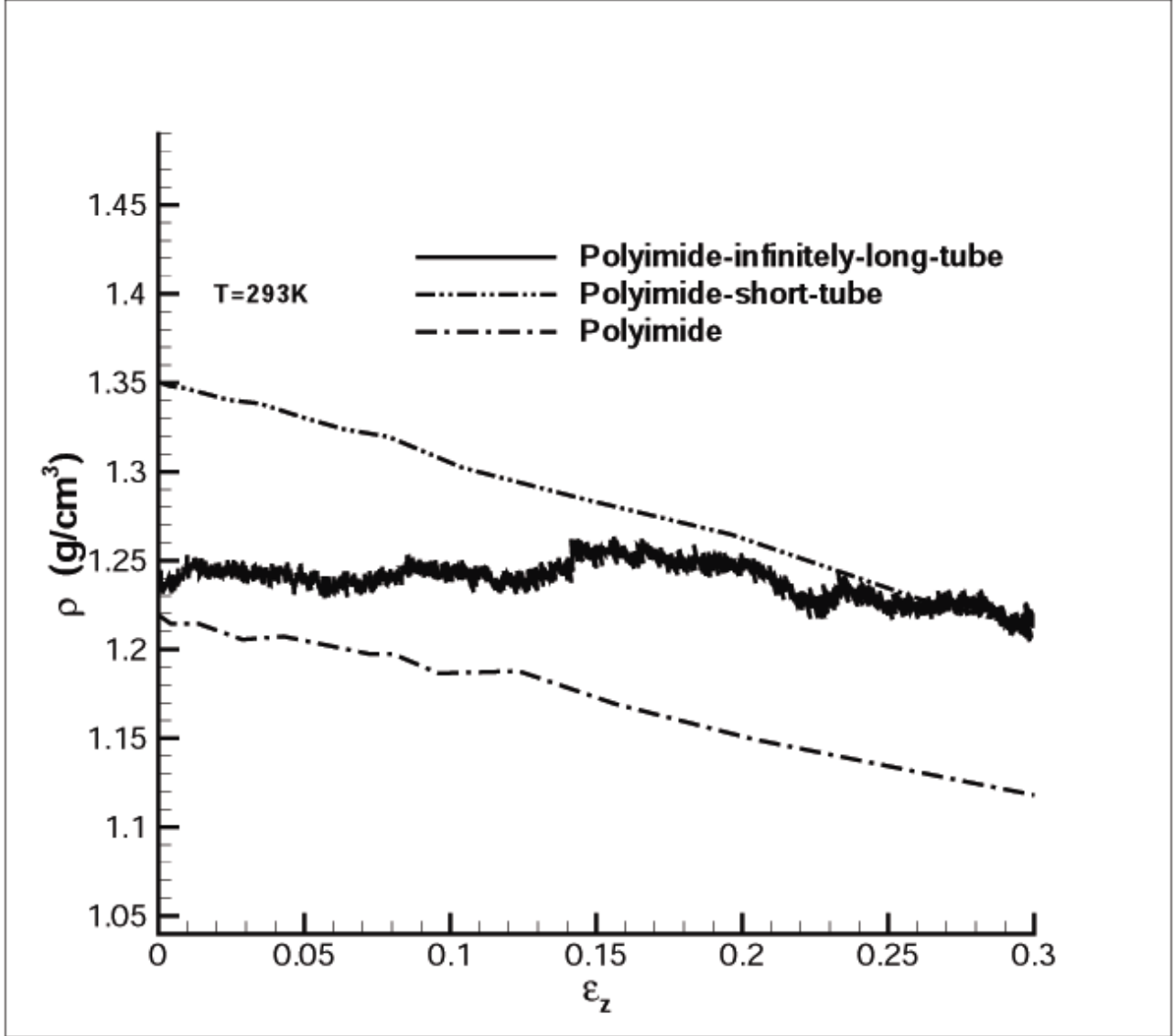


Figure 14. The densities as functions of strains  $\varepsilon_z$  for all three different composites during stretching.

When polymers are stretched in one direction, the polymers will simultaneously shrink in the other two directions, thus the Poisson ratio can be calculated during simulations. The Poisson ratio is defined by

$$\lambda_{zy} = -\frac{\varepsilon_y}{\varepsilon_z}$$

and can be estimated during stretching in the z-direction since the lengths of the simulation box are

variables in the simulations. The Poisson ratios are an average of three directions for isotropic composites. We obtain that the Poisson ratio is 0.35 for the polyimide composite at the room temperature. This result is comparable to the experimental results. The Poisson ratio  $\lambda_1 = 0.5(\lambda_{zx} + \lambda_{zy}) = 0.59$ , averaged from two transverse directions, for the infinite-long-tube composite. When the composite is stretched in the x-direction, it does not contract too much in the z-direction due to very stiff carbon nanotube placed in this direction. Thus, the Poisson ratio  $\lambda_2 = 0.5(\lambda_{xz} + \lambda_{yz}) = 0.0083$  is much smaller than  $\lambda_3 = 0.5(\lambda_{xy} + \lambda_{yx}) = 0.65$ .

## Conclusion

An aromatic polyimide and its mixtures with carbon nanotubes are prepared in a computer by using molecular dynamics simulation, repeated energy minimization and cooling processes. The stress-strain curves, Young's modulus, Poisson ratio and volumes are computed at different temperatures by using a constant tension algorithm in MD simulations. We find through the density-temperature curves that the glass transition temperature is 570 K for the model polyimide and 550 K for the polyimide-infinitely-long-tube composite. It is shown that the Young's modulus is increased 1.67 times by adding short carbon nanotubes at 36% by weight and that at the room temperature Young's modulus in the tube direction is increased 57 times by adding an infinitely long carbon nanotube of 16% composite in weight while Young's modulus in the transverse direction is increased 1.73 times. We also demonstrate that carbon nanotube can reduce the softening effect of temperature on mechanical properties and increase the ability to resist the deformation.

## Acknowledge

D. Qi appreciates the hospitality from National Institute of Aerospace and Structures and Materials Competency, NASA Langley Research Center during his sabbatical leave in 2003. Useful discussions with Drs. S.J.V. Frankland, G.M.Odegard, K. Wise, and C. Park are acknowledged. Computational time allocation on Cray T3E at the Pittsburgh Supercomputing Center through National Computational Science Alliance is appreciated.

## Reference:

1. Frankland, S.J.V.; Harik, V.M.; Odegard, G.M.; Brenner, D.W., and Gates, T.S., "The stress-strain behavior of polymer-nanotube composites from molecular dynamics simulation", *Composites Science and Technology*, 63, 1655-1661, (2003).
2. Bryant, R.G., "LARC-SI: a soluble aromatic polyimide. *High Perform. Polym.*, 8 (4) 607-615, (1996).
3. Hou, T.H, and Bryant, R.G, "Processing and properties of IM7/LARC-SI Polyimide Composites", *High Perform. Polym.*, 9, 437-448, (1997).
4. Park, C.; Ounaies, Z., Watson, K.A. Pawlowski, K, Lowther, S.E. Connell, J.W., Siochi, E.J., Harrison, J.S., St Clair, T.L., "Polymer-single wall carbon nanotube composites for potential spacecraft applications", NASA/CR-2002-211940, ICASE Report No. 2002-36
5. Fan, C.F. and Hsu, S.L. "Application of the Molecular Simulation Technique to Generate the Structure of an Aromatic Polysulfone System", *Macromolecules*, 24, 6244-6249, (1991).
6. Fan, C.F. and Hsu, S.L. "Application of the Molecular Simulation Technique to Characterize the Structure and properties of an Aromatic Polysulfone System. 2 Mechanical Thermal Properties", *Macromolecules*, 25, 266-270, (1992).
7. Fan, C.F., Cagin T., Chen, Z.M. "1. Force Field, Static Structure and Mechanical Properties", *Macromolecules*, 27, 2383-2391, (1994).
8. Clark, M., Cramer, R.D.C., and Opdenbosch, N.V., "Validation of the General Purpose Tripos 5.2 Force Field", *J Comp. Chem.* 10 (8) 982-1012 (1989).
9. Pinel, E., Brown, D., Bas, C., Mercier, R., Alberola, N.D., & Neyertz, S. "Chemical Influence of the Dianhydride and Diamine Structure on a Series of

- Copolyimides Studies by Molecular Dynamics Simulations”, *Macromolecules*, 35, 10198-10200, (2002).
10. S. J. Plimpton, S.J., “Fast Parallel Algorithms for Short-Range Molecular Dynamics”, *J. Comp. Phys.*, 117, 1-19 (1995).
  11. White, C.T., Robertson, and Minitmire, J. W., “Helical and rotational symmetries of nanoscale graphitic tubeles”, *Phys. Rev. B* 47, 5485-5488, (1993).
  12. Nose, S., *Mol. Phys.* 52 , 255 (1984).
  13. Hoover, W.G. “ Canonical Dynamics: equilibrium phase-space/distributions”, *Phys. Rev. A* 31 1695-1697, (1985).
  14. Brown, D. and Clarke, J.H.R. “Molecular Dynamics Simulation of an Amorphous Polymer under Tension. I. Phenomenology”, *Macromolecules*, 24, 2075-2082, (1998).
  15. Ray, J.R., “Elastic Constants and Statistical Ensembles in Molecular Dynamics”, *Computer Physics Reports*, 8, 109-152, (1988).
  16. Treacy, M.M.J.,Ebbesen, T.W. and Gibson, J.M. *Nature (London)* 382, 678 (1996).
  17. Hernandez, E., Subbaswamy, K.R., *Phys. Rev. Lett*, 80, 4502 (1998).
  18. Popov, V.N., Doren, V.E.V., Balkanski, M. “ Elastic properties of crystals of single-walled carbon nanotubes”, *Solid State Communications* 114, 395-399, (2000).
  19. Theodorou, D.N., and Suter, U.W., *Macromolecules*, 19, 139, (1986).
  20. Lee, M.N.; Whitley,K.S., and Gates,T.S, “ The Role of Molecular weight and temperature on the elastic and viscoelastic properties of a glassy thermoplastic polyimide”, *International J. Fatigue*, 24, 185-195, (2002).